Geometric control of kinetic pathways: Characterizing equilibrium in epitaxial growth

Paul N. Patrone[1,2],* Russel E. Caflisch[3],† and Dionisios Margetis[4‡]

[1]*Department of Physics, and Institute for Research in Electronics and Applied Physics,*
University of Maryland, College Park, Maryland 20742, USA
[2]*Center for Nanoscale Science and Technology, National Institute*
of Standards and Technology, Gaithersburg, Maryland 20899, USA
[3]*Department of Mathematics, and Institute for Pure and Applied Mathematics,*
University of California, Los Angeles, California 90095, USA and
[4]*Department of Mathematics, and Institute for Physical Science and Technology,*
and Center for Scientific Computation and Mathematical Modeling,
University of Maryland, College Park, Maryland 20742, USA
(Dated: August 30, 2011)

Using a kinetic model of epitaxial growth, we describe how geometry controls kinetic pathways through which external deposition influences the state of a vicinal surface. Three key, experimentally adjustable parameters, the local step angle θ, Péclet number P, and single bond detachment rate d, determine the state of the surface. By scaling arguments in P, we find three steady state regimes: In one regime, detailed balance approximately holds, so that the system is near equilibrium. In the other two regimes, geometric effects compete with deposition as the system is driven progressively out of equilibrium. Our analytical results are in excellent agreement with those of kinetic Monte Carlo simulations.

PACS number(s):

Epitaxial growth involves a competition between certain atomistic processes that disrupt detailed balance (DB) and others that tend to restore equilibrium [1]. In many systems, changing the local geometry activates kinetic pathways, thereby controlling how easily equilibrium can be reached. For example, the rates of some chemical reactions are increased by atomic defects that break the planar symmetry on platinum surfaces [2, 3].

In epitaxial systems, changes to the large scale morphology are driven in part by processes analogous to chemical reactions, namely, bond formation and breaking associated with attachment and detachment of atoms at step edges. [4, 5]. From this perspective, it is natural to ask: when is a crystal surface near equilibrium, and what role does the microscopic step geometry play in determining how far the system is from equilibrium?

Our goal in this Letter is to provide a criterion, in the context of a tractable model, that indicates when an epitaxial system is near equilibrium, as opposed to other *kinetic* steady states. Specifically, we address two tasks: (i) we define the state of the system (equilibrium or not) by means of analytical expressions for the kink density (number of atomic defects per unit length of a step); and (ii) we show how experimentally adjustable parameters, e.g. the local step angle θ and the Péclet number $P \propto F/D_e$, can control what state the system is in (F is the external deposition rate, and D_e is a diffusivity associated with atomic motion at a step). In particular, we show how increasing θ favors a return to equilibrium by creating additional kinks for adatoms to attach to.
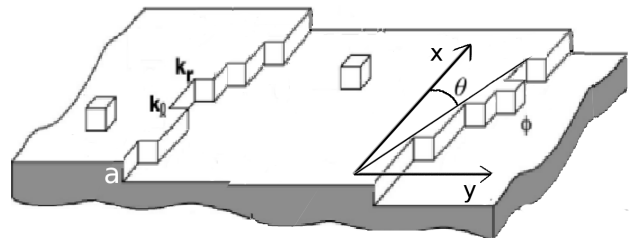
———

* ppatrone@umd.edu
† rcaflisch@ipam.ucla.edu
‡ dio@math.umd.edu

FIG. 1. Schematic of step geometry. The symbols ϕ and k_r (k_l) are the densities of edge adatoms and right (left) facing kinks, respectively. The local step angle is θ.

Our work is motivated by the issue of how accurately experimental surface systems can be described by near-equilibrium theories based on the celebrated Burton-Cabrera-Frank (BCF) model [5–8]. By starting with a more general kinetic model, which contains information about kinks, we aim to provide some insight into the conditions necessary for the validity of BCF-type theories.

We adopt a modified version of the mean field, step-edge model in [9, 10], which describes surfaces in and out of equilibrium see also [11] for related works). Features of our model are depicted in Fig. 1, which shows two steps separated by a terrace on a typical crystal surface [4, 5]. The steps have atomic height a, and atoms are deposited on the surface at rate F. Adsorbed atoms (adatoms) diffuse on terraces, and may attach to and detach from step edges [5]. For our present purposes, it suffices to study a single step on a simple cubic lattice. At a step edge, we distinguish between edge, kink, and boundary adatoms, which have one, two and three nearest in-plane neighbors, respectively. The densities of edge and kink adatoms are ϕ and k. Kinks can be right or left facing, with densities k_r and k_l (cf. Fig. 1).
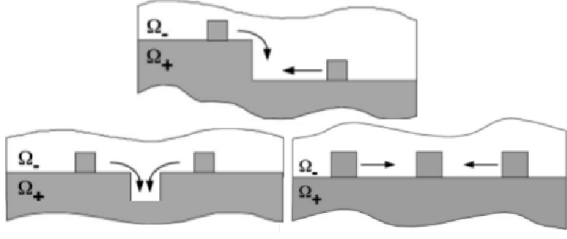
FIG. 2. Top down view of the processes by which a step moves locally. The symbol Ω_+ (Ω_-) denotes the upper (lower) terrace at a step edge. Starting from the top and going clockwise, the coordination numbers for these processes are $c_1 = c_2 = c_3 = 2$; cf. Eqs. (2) and (3).

Morphological changes to the surface occur via step motion, which in turn results from atomistic processes that create and destroy kinks [4]. Specifically, to advance a step locally, an edge adatom must either (i) attach to an existing kink, (ii) form a left-right kink pair by attaching to another edge adatom, or (iii) annihilate a right-left kink pair (cf. Fig. 2) [9, 10]. The reverse processes cause steps to retreat.

We identify equilibrium as the state in which *detailed balance* (DB) holds for all atomistic processes causing step motion [12, 13]. By detailed balance, we mean that the net rate of any process (the product of a single particle transition rate and the density of atoms eligible to make that transition) equals the net rate of its reverse process [9, 14]. The kink density plays a *central* role in determining when the system is near equilibrium, since k connects kinetic processes to the local step geometry.

Therefore, we begin our analysis by writing

$$k_r + k_l = k, \qquad k_r - k_l = a^{-1}\tan\theta, \qquad (1)$$

Assuming that steps are straight on average, we take θ to be spatially constant along the step edge. We also take the edge adatom (ϕ) and kink (k) densities to be spatially constant, so that they obey

$$\partial_t \phi = FL + c_1(a^{-2}D_k k - a^{-1}D_e \phi k), \qquad (2)$$
$$\partial_t k = c_2 a^{-1}(D_e \phi^2 - D_k k_r k_l) + c_3(a^{-3}D_b - D_e \phi k_r k_l), \qquad (3)$$

where L is the average terrace width, and D_e, D_k, and D_b are the diffusivities of edge, kink, and boundary adatoms [9, 10]. The constants c_1, c_2, and c_3 are coordination numbers measuring the number of pathways by which edge adatoms and kinks can be created or destroyed (cf. Fig. 2).

Equations (2) and (3) are simplified versions of the evolution equations given in [9, 10]. The right-hand side of Eq. (2) states that (i) all deposited adatoms move to a step edge (via the term FL), (ii) atoms detach from kink sites with probability k at a rate D_k, and (iii) edge adatoms attach to kink sites with probability ϕk at a rate D_e. The term c_1 in Eq. (2) indicates that the processes of adatom detachment-attachment at a kink site occur by c_1 different pathways. Equation (3) and the coefficients c_2 and c_3 can be interpreted similarly (cf. Fig. 2).

We assume that the diffusion coefficients [15] are

$$D_\ell = D_T \exp(-E_\ell/k_B T), \qquad (4)$$

where D_T is the diffusion coefficient for adatoms on a terrace, $\ell = e, k,$ or b for edge, kink, or boundary adatoms, and $E_\ell = n_\ell E_{\text{bond}}$; E_{bond} is the energy of a single atomic bond, and n_ℓ is the number of nearest in-plane neighbors of a given adatom type [4, 9]. Note that $n_\ell = 1, 2$ or 3 for $\ell = e, k,$ or b. We also define the single bond detachment rate $d = D_k/D_e = D_b/D_k = \exp(-E_{\text{bond}}/k_B T)$.

We look for steady states by setting the time derivatives equal to zero in Eqs. (2) and (3), so that

$$P = c_1(a^2 \phi k - adk), \qquad (5)$$
$$c_2 a^2 (dk_r k_l - \phi^2) = c_3(d^2 - a^3 \phi k_r k_l). \qquad (6)$$

The parameter $P = aLF/(D_e/a^2)$ represents a competition between two atomistic processes; the numerator, aLF, is the flux of deposited adatoms arriving at a step edge, which drives the system *out of equilibrium*, since it violates DB [14]. The denominator, D_e/a^2, is the rate at which edge adatoms diffuse (i.e., hop) along a step edge. This diffusion is the fastest process by which the system may re-equilibrate. Hence, P should help control how close the system is to equilibrium. In this study we assume that $P \ll 1$ and $d \ll 1$, which corresponds to a regime in which the adatom density ϕ is low.

We begin by considering the case $F = 0$ (i.e., $P = 0$), so that Eqs. (5) and (6) imply $\phi = d/a$ and $k_r k_l = d/a^2$. Then, by Eq. (1),

$$k = a^{-1}(\tan^2\theta + 4d)^{1/2}. \qquad (7)$$

This is an equilibrium solution, since it satisfies DB; i.e., $D_k k = aD_e \phi k$, $D_e \phi^2 = D_k k_r k_l$, and $D_b = a^3 D_e \phi k_r k_l$ (cf. Eqs. (2) and (3)).

In Eq. (7), the terms in parentheses reveal two distinct sources of kinks. The term $a^{-2}\tan^2\theta = (k_r - k_l)^2$ corresponds to *geometric* kinks; these arise solely from the non-zero step angle and all face the same direction (for example, if $\theta > 0$, then $k_r > k_l$, and geometric kinks are right facing). The term $4d$ is associated with *thermal* kinks, which are created when adatoms detach from kinks or edges and attach to each other. Thermal kinks always come in left-right pairs and do not contribute to the average step angle. When the single bond energy becomes large ($d \to 0$), detachment processes rarely occur, and the equilibrium kink density is given by the geometric kink density ($k \to |\tan\theta|/a$).

For nonzero P, it is convenient to rescale variables, letting $l = ak/d^{1/2}$, $q = P/d^{3/2}$, and $\psi = \tan(\theta)/d^{1/2}$. Algebraic manipulations of Eqs. (5) and (6) then yield

$$c_1^2 [c_3 + c_2] l^4 + c_1 c_3 q l^3 - c_1^2 [c_3 + c_2](4 + \psi^2)l^2$$
$$- c_1 [c_3 \psi^2 + 8c_2] ql - 4c_2 q^2 = 0. \qquad (8)$$

This fourth-order algebraic equation for l (i.e., for k) can be solved exactly, but we resort to approximations that are more useful for physical interpretation. There are

three distinct regimes in which the solution to Eq. (8) may be simplified: (i) $q \ll (1+\psi^2)^{1/2}$; (ii) $(1+\psi^2)^{1/2} \ll q \ll (1+\psi^2)^{3/2}$; and (iii) $(1+\psi^2)^{3/2} \ll q$. Note that regime (ii) only exists if $1 \ll |\psi|$, so that it could be rewritten as (ii') $|\psi| \ll q \ll |\psi|^3$. The kink density k solving Eq. (8) is found approximately in these three regimes to be

$$k \approx a^{-1}(\tan^2\theta + 4d)^{1/2}, \qquad P \ll d(d+\tan^2\theta)^{1/2} \quad (9)$$
$$k \approx a^{-1}|\tan\theta|, \qquad d|\tan\theta| \ll P \ll |\tan\theta|^3 \quad (10)$$
$$k \approx a^{-1}[4c_1 P/(c_2 c_3)]^{1/3}, \qquad (d+\tan^2\theta)^{3/2} \ll P. \quad (11)$$

In Eq. (9), the kink density is approximately equal to the value given by Eq. (7); corrections to Eq. (9) are of order P. We call this the "*near-equilibrium*" (NE) regime, since DB is approximately satisfied; indeed the dominant balance in Eq. (5) is $a^2\phi k \approx adk \gg P$.

Equation (11) corresponds to a state in which information about the step angle θ is lost; the kink density is entirely determined by the Péclet number. Since the presence of P in Eq. (11) implies that deposition determines the kink density, we call this regime the "*flux dominated steady state*" (FDSS). DB is lost in this kinetic steady state. The flux to the edge is balanced by flux of edge adatoms to kinks. The creation of kink pairs from two edge adatoms is balanced by the hopping of an edge adatom to fill in a single missing atom in the edge (a kink pair), as illustrated in Fig. 2; i.e., Eqs. (5) and (6) imply

$$c_1 a^2 \phi k \approx P, \qquad (12)$$
$$c_2 \phi^2 \approx c_3 a\phi k_r k_l. \qquad (13)$$

In the intermediate regime governed by Eq. (10), which we call the "*angle-dominated steady state*" (ADSS), kinks are predominantly geometric. For example, if $\theta > 0$, then $k_r \gg k_l$, so that $k_r \approx a^{-1}|\tan\theta|$. A higher order correction yields $k_l \approx a^{-1}c_2 P/(c_1 c_3 \tan^2\theta)$. This correction term for the ADSS is determined by the dominant kinetic balances, Eqs. (12) and (13) as in the FDSS.

Although the ADSS does not satisfy DB, it may be interpreted as an extension of the NE regime: the ADSS amounts to an increase (relative to the NE regime) of the range of d and P values for which the kink density is approximately independent of the deposition rate. As d decreases (keeping $P, \theta \neq 0$ fixed) in the NE regime, the system transitions *continuously* from NE to the ADSS (cf. Fig. 3). If instead P and d are held fixed, increasing θ can eliminate the flux dependence of k (cf. Fig. 4).

The ADSS kink density is controlled by the step angle alone (and not P or d) because *geometric* kinks inhibit the formation of left-right kink pairs. This can be seen by considering the length $\tilde{a} = a/\tan\theta$ and time $\tilde{t} = \tilde{a}^2/D_e$, which are the average length between geometric kinks and the average time for a single edge adatom to traverse the distance $\tilde{a}$. Rewriting the ADSS condition $P \ll |\tan^3\theta|$ (cf. Eq. (10)) in the form $\tilde{t} \ll (\tilde{a}LF)^{-1}$ and noting that $1 \ll |\psi|$ is equivalent to $\tilde{t} \ll a^2/D_k \ll a^2/D_b$ suggests that an edge adatom attaches to an adjacent geometric kink long before another edge adatom is created
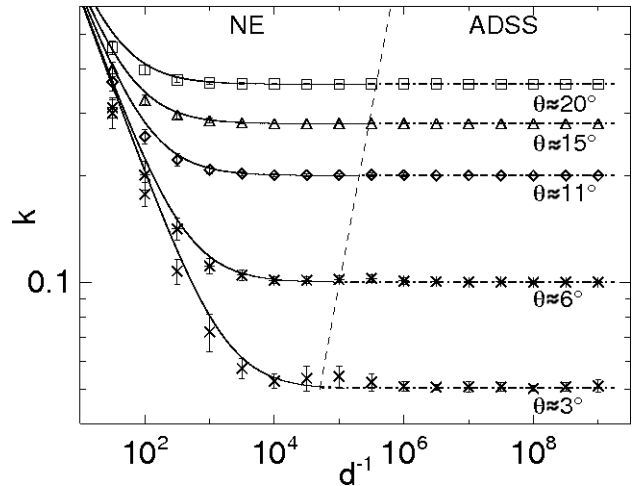

FIG. 3. KMC-simulated kink densities (symbols with error bars) versus Eqs. (9) and (10) (solid and dash-dot lines, respectively). The slanted dashed line indicates the approximate boundary between the NE and ADSS regimes; it is the solution to $P = d|\tan\theta|$. We fixed $P = 10^{-6}$ for these simulations. The ADSS kink density exhibits the same behavior as the NE kink density taken in the limit $d \to 0$.

within a distance $\tilde{a}$ by either deposition or detachment. Thus, in the ADSS, geometric kinks shield edge adatoms from each other, so that left-right pairs rarely form.

In order to test our analytical results, we performed kinetic Monte Carlo (kMC) simulations of a cubic, solid-on-solid surface model. Details of the algorithm may be found in [16, 17]. The main idea is to move adatoms with probabilities proportional to their diffusion rates, given by Eq. (4). We modeled the surface on a $500\,a \times 200\,a$ rectangular grid, whose sides were parallel to the x and y axes of the crystal (cf. Fig. 1). The surface was initialized to have four steps separated by terraces 50 atomic lengths wide. The x axis corresponded to $\theta = 0$ (cf. Fig. 1). Nonzero step angle was incorporated by applying screw periodic boundary conditions along lines making an angle θ with the x-axis; realizable values of θ for this simulation were those satisfying $\tan\theta = j/500$ for some integer j.

We compare simulated kink densities with the analytic predictions from Eqs. (9)-(11), as a function of d in Fig. 3 and as a function of P in Fig. 4. Both figures show excellent agreement between the model predictions and the results from kMC simulations in all three regimes. This is true even for kink densities k of size up to 0.4, which is somewhat surprising, since we do not expect our mean-field model to be valid when any density becomes comparable to unity (i.e., adatom and kink correlations could significantly alter the form of Eqs. (2) and (3)). Morever, Fig. 3 confirms our conclusion that the ADSS exhibits NE behavior, since it shows that the NE kink density approaches the ADSS kink density as d becomes small. Also, Fig. 4 confirms that the kink density is approximately independent of the step angle in the FDSS regime (i.e., to the right of the red bar on each curve).

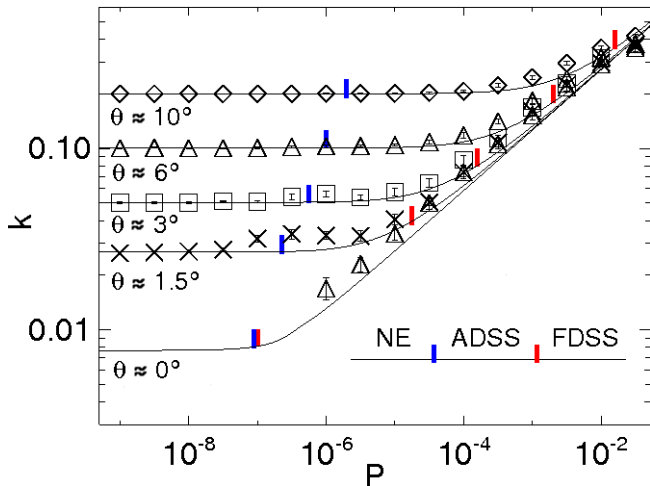Our model does not take into account island forma-

FIG. 4. [Color Online] Analytic (solid lines) and kMC (symbols) kink densities as functions of P. Analytic densities were found by numerically solving Eq. (8). The kink densities collapse to a single curve as P increases. For each θ, blue and red vertical lines indicate the locations of the NE to ADSS and ADSS to FDSS transitions, going left to right. We omit NE kMC data for $\theta = 0$; significantly larger simulations are required to suppress fluctuations in this data. We set $d = 10^{-5}$ and disabled island nucleation in these simulations.

tion; this process will decrease the magnitude of P (via FL), since not all of the deposited adatoms will diffuse to a step edge. More generally, we ignore the effects that terrace inhomogeneities (e.g. islands) have on a step.

We believe that our analytical results, Eqs. (9)–(11), are experimentally testable by means of molecular beam epitaxy (MBE) and *in situ* scanning-tunneling microscopy (STM). For example, certain STM designs permit atomic resolution imaging of Si(111) surfaces *during growth* [18, 19]. Since diffusion rates are functions of temperature [4], and the deposition rate can be controlled during MBE, P and d correspond to experimentally adjustable parameters. Therefore, we expect that it should be possible to experimentally observe the active kinetic processes implied by the dominant balances in Eqs. (5) and (6).

In conclusion, we presented a mean field model of epitaxial growth to demonstrate how varying the step angle θ, deposition rate $F \propto P$, and single bound detachment rate d, determine whether a vicinal surface is in equilibrium or in a non-equilibrium steady state. We showed that the system has three steady-state regimes. In one regime, the system obeys detailed balance and is near equilibrium. In the other two regimes, the behavior of the system is determined by θ and P, respectively. Our analysis is in excellent agreement with kMC simulations in all three regimes. We hope that our characterization of active kinetic processes in surface systems can be further explored by STM measurements during growth.

[1] J. W. Evans, P. A. Thiel, and M. C. Bartelt, Surf. Sci. Rep. **61**, 1 (2006).
[2] G. A. Somorjai and D. W. Blakely, Nature **258**, 580 (1975).
[3] S. Ferrer, J.M. Rojo, M. Salmeron, G.A. Somorjai, Philos. Mag. A (Phys. Condensed Matter Defects Mech. Properties) **45**, 261 (1982).
[4] H.-C. Jeong and E. D. Williams, Surf. Sci. Rep. **34**, 171 (1999).
[5] W. K. Burton, N. Cabrera, and F. C. Frank, Phil. Trans. R. Soc. London A **243**, 299 (1951).
[6] O. Pierre-Louis and C. Misbah, Phys. Rev. B **58**, 2259 (1998).
[7] R. Ghez, H. Cohen, and J. Keller, J. Appl. Phys. **73**, 3685 (1993).
[8] F. Liu and H. Metiu, Phys. Rev. E **49**, 2601 (1997).
[9] R. E. Caflisch, W. E, M. F. Gyure, B. Merriman, and C. Ratsch, Phys. Rev. E. **59**, 6879 (1999).
[10] D. Margetis and R. E. Caflisch, Multiscale Model. Simul. **7**, 242 (2008).
[11] L. Balykov and A. Voigt, Phys. Rev. E **72**, 022601 (2005); L. Balykov and A. Voigt, Multiscale Model. Simul. **5**, 45 (2006); R. E. Caflisch and B. Li, Multiscale Model. Simul. **1**, 150 (2003); S. N. Filimonov and Yu. Yu. Hervieu, Surf. Sci. **553**, 133 (2004); and J. Kallunki and J. Krug, Surf. Sci. Lett. **523**, L53 (2003).
[12] J.-F. Gouyet, M. Plapp, W. Dieterich and P. Maass, Adv. Phys. **52**, 523 (2003).
[13] R. K. P. Zia and B. Schmittmann, J. Stat. Mech. **2007**, P07012 (2007).
[14] Deposition-induced step growth violates DB, since processes that cause steps to advance in y (cf. Fig. 1) occur at a faster net rate than those that cause steps to retreat.
[15] The products $a^2 D_\ell$ can be thought of as hopping rates for adatom moves between lattice sites.
[16] J. G. Amar, Comput. Sci. Eng. **8**, 9 (2006).
[17] A. F. Voter, in *Radiation Effects in Solids*, NATO Science Series, edited by K. E. Sickafus, E. A. Kotomin, and B. P. Uberuaga (Springer, Dordrecht, 2007).
[18] B. Voigtländer and A. Zinner, Appl. Phys. Lett. **63**, 3055 (1993); B. Voigtländer, A. Zinner, and Th. Weber, Rev. Sci. Instrum. **67**, 2568 (1996).
[19] B. Voigtländer, M Kästner, and P. Šmalauer, Phys. Rev. Lett. **81**, 858 (1998).